Food Chemistry xxx (xxxx) xxx

Contents lists available at ScienceDirect

Food Chemistry

journal homepage: www.elsevier.com/locate/foodchem

Quartz crystal microbalance sensor based on 11-mercaptoundecanoic acid self-assembly and amidated nano-titanium film for selective and ultrafast detection of phosphoproteins in food

Jianping Guo [a], Guozhen Fang [a], Shuo Wang [b], Junping Wang [a,*]

[a] Key Laboratory of Food Nutrition and Safety, Ministry of Education, Tianjin University of Science & Technology, 29 The Thirteenth Road, Tianjin Economy and Technology Development Area, Tianjin 300457, PR China
[b] Medical College, Nankai University, No.38 Tongyan Road, Jinnan District, Tianjin 300350, PR China

ARTICLE INFO

Keywords:
Phosphoproteins
Quartz crystal microbalance sensor
Aminated nano-titanium dioxide
Ultrafast determination
Food

Chemical compounds studied in this article:
11-Mercaptoundecanoic acid (PubChem CID: 543502)
N-(3-dimethylaminopropyl)-N'-ethylcarbodiimide (PubChem CID: 2723939)
N-Hydroxysuccinimide (PubChem CID: 80170)
Trifluoroacetic acid (PubChem CID: 6422)
2,5-Dihydroxybenzoic acid (PubChem CID: 3468)
Ethanol (PubChem CID: 702)
Acetic acid (PubChem CID: 176)

ABSTRACT

A novel quartz crystal microbalance (QCM) sensor for trace-phosphoprotein ultrafast detection was constructed based on the bridge interactions between the NH_2-TiO_2 sites enriched on Au-electrode and phosphate groups. Herein, 11-mercaptoundecanoic acid (MUA) modified by Au-S bond acted as carrier for immobilizing NH_2-TiO_2. Functionalized NH_2-TiO_2 to absorb phosphoproteins. Under the optimal conditions, the proposed sensor showed a linear frequency shift to the concentration of α-casein ranging from 1.0×10^{-3} to 1.0 mg mL^{-1} with a low detection limit of 5.3×10^{-6} mg mL^{-1} (S/N = 3), and the limit of quantitation was 0.001 mg mL^{-1}. Compared with traditional Ti^{4+}-IMAC/MOAC-system, the analysis process of NH_2-TiO_2/MUA/AuE-QCM sensor was simpler and faster which could complete within 5 min. Additionally, the constructed biosensor was successfully used for the non-fat milk and chicken egg white. This proposed sensor presents a great prospective strategy for the evaluation of the nutrition in different foods.

1. Introduction

Protein phosphorylation is a very important post-translational modification in addition to glycosylation, methylation, acetylation (Tramutola, Lanzillotta, Perluigi, & Butterfield, 2017), etc. Phosphorylation affects gene expression and activities of regulatory cellular (Gruhler et al., 2005; Hunter, 1995; Manning, Whyte, Martinez, Hunter, & Sudarsanam, 2002). At present, phosphorylation is often used as an effective method to improve the functional properties of food proteins. It has health benefits, such that phosphorylated proteins can effectively improve the body's absorption of calcium and human immunity as well as its good antioxidant effect on lipids(Lebetwa, Suzuki, Tanaka, Nakamura, & Katayama, 2019; Li, Enomoto, Hayashi, Zhao, & Aoki, 2010). A marked increase in solubility, emulsification and emulsification stability was observed when native peanut protein was phosphorylation-modified by sodium tripolyphosphate (Yu et al., 2015). Li Wang (Chen et al., 2019) also proved phosphorylated wheat gluten proteins had better solubility, emulsifying-property and foamability; the thermal stability and calcium-binding capacity of ovalbumin can be improved by dry heat-phosphorylation (Li, Chen, Peng, Enomoto, Hayashi, Li et al., 2010; Twisk, 2013). In terms of physiological function, phosphorylated-β-LG, α-LA and bovine serum proteins have weaker antigenicity than all-non-phosphoproteins, as verificated by Enomoto et al. (2007). Therefore, it is conceivable that the moderate intake of phosphoproteins was better for human health. However, the amount of phosphoprotein is not same in different foods and the aberrant phosphorylation may be one of the potential factors for signs of cancer, diabetes, chronic inflammation, or neurodegenerative diseases (Chen et al., 2017; Zanivan et al., 2008). Thus, the fast and convenient analysis method for phosphoprotein is very important for evaluating the

* Corresponding authors.
E-mail address: wangjp@tust.edu.cn (J. Wang).

https://doi.org/10.1016/j.foodchem.2020.128656
Received 12 March 2020; Received in revised form 12 November 2020; Accepted 12 November 2020
Available online 18 November 2020

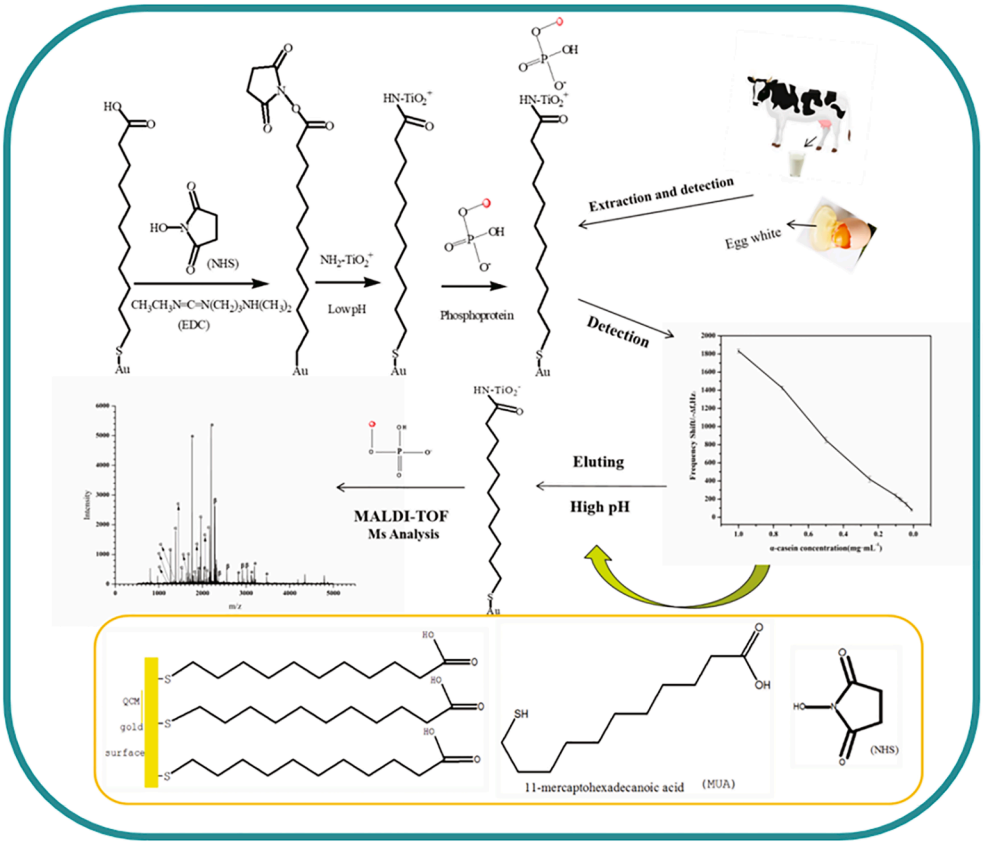

Scheme 1. The preparation of NH_2-TiO_2/MUA/AuE-QCM sensor and the detection process of phosphoproteins.

nutrition of food.

To date, various techniques have been developed for the detection of phosphoproteins, including mass spectrometry, fluorescence, marked radio-isotopes, immunoassay approaches and electrochemistry (Gao, Wang, Wang, & Xia, 2016; Zhang et al., 2013). Among these methods, laser desorption ionization-time-of-flight mass spectrometry (MALDI-TOF/MS) is most commonly used due to its sensitivity and reliability, but there still exist some disadvantages such as expensive instruments, tedious sample preparation and time-consuming analysis procedure, which reduce the detection efficiency of phosphoproteins. To overcome these disadvantages, it is urgent to develop a novel strategy for phosphoproteins analysis. The detection technology of phosphoproteins based on quartz crystal microbalance (QCM) sensors have not been reported yet.

QCM, as a kind of mass-sensitive detector at nanogram levels, has been widely applied in various fields, including bioscience, immunoassay, environmental and food analysis due to its advantages of rapidity, extreme sensitivity and simple operation (Kong et al., 2014; Pan et al., 2013). However, the unmodified quartz crystal microbalance has no specificity for different molecules (Say, Gultekin, Ozcan, Denizli, & Ersoz, 2009). Outstanding selectivity can be realized by modifying specific functional materials on the surface of QCM sensor as recognition element (Avila, Zougagh, Escarpa, & Rios, 2007). As it is well known, the stability of material-electrode binding, the thickness of membrane and the transducer surface of the sensor can directly affect the performance of sensor. In Zhao's work(Zhao, He, Wang, Wang, & Wang, 2020), the proposed method utilized the traditional molecularly imprinted polymers (MIPs) as the recognition elements and methimazole as template molecule, in which imprinted polymers performed high selectivity, yet slow transfer, small binding capacity, or even leakage of template molecules (Haupt, Medina Rangel, & Bui, 2020). In addition, a time-consuming MIP-film be generated adjacent to the Au-electrode surface result in blocking a large portion of the electroactive surface area. Moreover, macromolecules proteins are generally more difficult produced for MIP than smaller molecular targets (for example, 1-methyl-2mercaptoimidazole, MMZ). To a certain extent, the applications of MIP are limited. Recently, self-assembling is a simple and effective method to prepare specificity membrane on the transducer surface of QCM sensor. In this study, aminated nano-titanium film self-assembled on AuE serving as an identification element for trace phosphoproteins, which provided not only specific selectivity but also a large surface area and a high mass-transfer rate. This functional nano-material recognition, in combination with modern sensing techniques QCM to monitor changes in the recognition targets, offers the promise of selective, sensitive sensors capable of detecting and online-testing analytes in a non-labeling way.

Nano-TiO_2, a vital member of the phosphoprotein-enrichmented material family, has drawn significant interest due to its excellent performance such as high specific surface areas, excellent thermal/mechanical stability and its specific and reversible chemisorption of phosphate groups on their amphoteric surface. TiO_2 is positively charged as a Lewis acid under acidic conditions, which can form an electrostatic attraction with the phosphate of the anion and combine with each other; under alkaline conditions, it will be separated from the phosphoproteins as a Lewis base (Lu, Duan, He, Hu, & Yin, 2010; Ma et al., 2012), so it can selectively enrich trace phosphoproteins. However, the poor hydrophilicity of TiO_2 greatly reduces its ability to selectively adsorb phosphoproteins with higher hydrophilicity. In addition, the higher Lewis acidity of TiO_2 makes it more easily to adsorb the non-phosphoproteins.

TiO_2 bond distances are small and unequal which makes the polarity of the molecules very strong. The strong polarity can make the surface easily absorb water molecules, further polarizing to form surface hydroxyl groups which make it easy to be modified in surface under the

special structure. Therefore, it can be used as a generalized base combined with modifiers to complete its surface modification (Baker et al., 2011). Amino-functionalized (NH_2-TiO_2) has stronger specific adsorption for phosphoproteins due to its lower Lewis acidity and higher hydrophilicity. The aminated nano titanium dioxide has a particle size of 5 nm, which is characterized by high purity, good dispersibility and large surface activity. It was reported, Dai (Dai, Wang, & Liu, 2017) firstly has synthesized a novel immobilized metal affinity chromatography (IMAC) material with DOTA(1,4,7,10-tetraazacyclododecane *N,N′,N″, N‴*-tetraacetic acid) coated on the surface of NH_2-TiO_2 (Zr^{4+}(TiO_2@DOTA-Zr) to improve the enrichment specificity and sensitivity for phosphopeptides successfully. NH_2-TiO_2 nanomaterials were chosen as a support matrix, which would offer a high specific surface area and good hydrophilia to provide an additional selectivity for enriching phosphopeptides.

Inspired by above explorations, an "all-in-one" type QCM-sensor for detection of phosphoproteins was constructed to validate the proposed strategy. Compared to MS-method (Hong et al., 2018; Zhu et al., 2019), this proposed technology integrates all step-analysis steps (including online enrichment, separation and detection) together. It can simultaneously enrich and detect the phosphoproteins containing a number of proteins and high levels of urea and salts. Moreover, it provides time-saving, simplified test-process via QCM analysis without complicated multi-step enrichment procedures of up to 60 min or longer reported (Hussain et al., 2013; Wang, Zhang, Sun, & Ni, 2014). In addition, there has been much success in MS-method, but the detection of phosphoproteins by electrochemical-method is sporadic in the literature, especially from a complex biological sample. In 2016 (Gao et al., 2016), although an electrochemical sensor based on ZrO_2 film were being employed to detect phosphopeptides and overcoming the shortcoming of time-consuming, yet the sensitivity (LOD: 0.09 mM) of ZrO_2-sensor was low. Thus, our technology increase analysis efficiency of the phosphoproteome and may further provide significant information for the functional foods.

Herein, for the first time, a novel QCM sensor was fabricated for the phosphoproteins rapid determination by using NH_2-TiO_2 nanomembrane as a recognition element on Au electrode (AuE) surface modified with 11-mercaptoundecanoic acid. To the best of our knowledge, this is the first attempt to modified functional NH_2-TiO_2 nanomateril on the transducer surface to construct QCM sensor for the detection of phosphoproteins. NH_2-TiO_2 was used to increase the effective adsorbed sites and thus amplify the frequency response signal, by increasing effective surface area on the electrode and enhancing effectiveness of the self-assembly process. This research was aimed at overcoming some shortcomings of time-consuming, complicated pretreatment process of mass spectrometric analysis, and also offering an ultrafast, selective, simple, reproducible and stable QCM sensor for online enrichment and detection of phosphoproteins in real samples. The NH_2-TiO_2/MUA/AuE-QCM sensor construction and detection process is outlined in Scheme 1.

2. Materials and methods

2.1. Materials and chemicals

11-Mercaptohexadecanoic acid (MUA), *N*-hydroxysuccinimide (NHS) N-(3-dimethylaminopropyl)-N'-ethylcarbodiimide(EDC), and carbonate buffered saline (NH_4HCO_3, 50 mmolL^{-1}, pH 6.5) were brought from Sigma-Aldrich (USA). Trypsin, β-Casein, α-Casein, Casein, Bovine serum albumin (BSA), Lactoglobulin, Lactoferrin, Whey protein all these proteins were bought from Sigma-Aldrich (USA). Aminated nano titanium dioxide was purchased from Liuzhou Nanometer Material Co. Ltd (Guangzhou, China). Trifluoroacetic acid (TFA) and 2,5-dihydroxybenzoic acid (2,5-DHB) was obtained from Sigma-Aldrich (St. Louis, MO, USA). Non-fat milk and chicken eggs were brought from a local supermarket (TESCO Tianjin). All aqueous solutions were prepared using Milli-Q water by Milli-Q purification system (Millipore, Milford, MA, USA). All other chemicals and reagents were of the highest grade commercially available.

2.2. Instruments and electrodes

A QCA922 quartz crystal analyzer (Princeton Applied Research, Oak Ridge, TN, USA) was used to monitor frequency change(Δf) in real time during aminated nano titanium dioxide immobilization, phosphoproteins adsorbing.

All electrochemical experiments were performed using a PARSTAT 2273 electrochemistry workstation (Princeton Applied Research, USA) coupled with a QCM (QCM-922, Princeton Applied Research, USA) equipped with a commercial 9 MHz AT-cut quartz crystal coated with AuE (area 0.196 cm^2) on both sides (Seiko EG&G). In the experiments, the quartz crystal was mounted into the Teflon holder (well-type, QA-CL3, Seiko EG&G) to ensure that only one side of the AuE was exposed to the solution. All electrochemical experiments were performed with a conventional three-electrode system, consisting of a bare or modified quartz crystal AuE as the working electrode, a saturated calomel electrode as the reference electrode, and a platinum column electrode as the counter electrode. QCM was also used to record the frequency change of the quartz crystal AuE. The surface morphologies of electrodes were characterized by atomic force microscope (AFM, SUPRA 55 sapphire Germany). MALDI-TOF MS (Bruker, Germany) was utilized to qualitatively validate the accuracy of the results from sensor.

2.3. Preparation of NH_2-TiO_2/MUA/AuE

Prior to modification, the bare AuE of quartz crystal was ultrasonically washed with ethanol and then cleaned with freshly prepared "piranha" solution (30% H_2O_2/H_2SO_4 = 1:3, v/v) for 5 min. After rinsing with ultra-pure water and ethanol, the crystal was blown dry with a gentle flow of pure nitrogen gas and mounted into the well.

(A) 11-mercaptoundecanoic acid self-assembly on the AuE: the electrode was soaked in an ethanol solution of 0.01 mol·L^{-1} 11-mercaptoundecanoic acid for overnight reaction. On the surface of the quartz crystal gold electrode, a carboxyl-terminated thiol monolayer (Ding et al., 2013) was formed directly through the Au-S bond, which served as a surface functionalization. The self-assembled QCM electrodes were washed three times with ethanol and ultrapure water, respectively, to remove unbound thiol undecanoic acid on the surface of the gold electrode and then stored in absolute ethanol. It should be blown dry with N_2 before use.

(B) Activation: 10 μL of the EDC and NHS mixed solution (0.4 mol L^{-1} EDC/0.1 mol L^{-1} NHS = 1:1, v/v) was added to the surface of the self-assembling electrode and reacted in the dark for 2 h. After the reaction, the surface of the electrode was washed with ultrapure water three times and blown dry by nitrogen for use. This activation process causes the carboxyl group on the surface of the electrode to be replaced by an ester group (Altintas, Uludag, Gurbuz, & Tothill, 2012).

(C) Connection of NH_2-TiO_2: on the surface of the electrode obtained above, 10 μL of aqueous amidated nano-titanium oxide solution was added, and it took 20 min to modify the electrode, then rinsing with water and drying with nitrogen at room temperature.

(D) Closing site: on the surface of the electrode obtained above, 10 μL of a 1% solution of BSA was added to block the carboxyl site of the unbound aminated nano titanium dioxide for 1 h. After that, it was washed twice with ammonium bicarbonate buffer and ultrapure water and dried with nitrogen, storing at 4 °C for use.

2.4. Measurement experiments

The frequency value (Δf_0, Hz) was recorded after the response

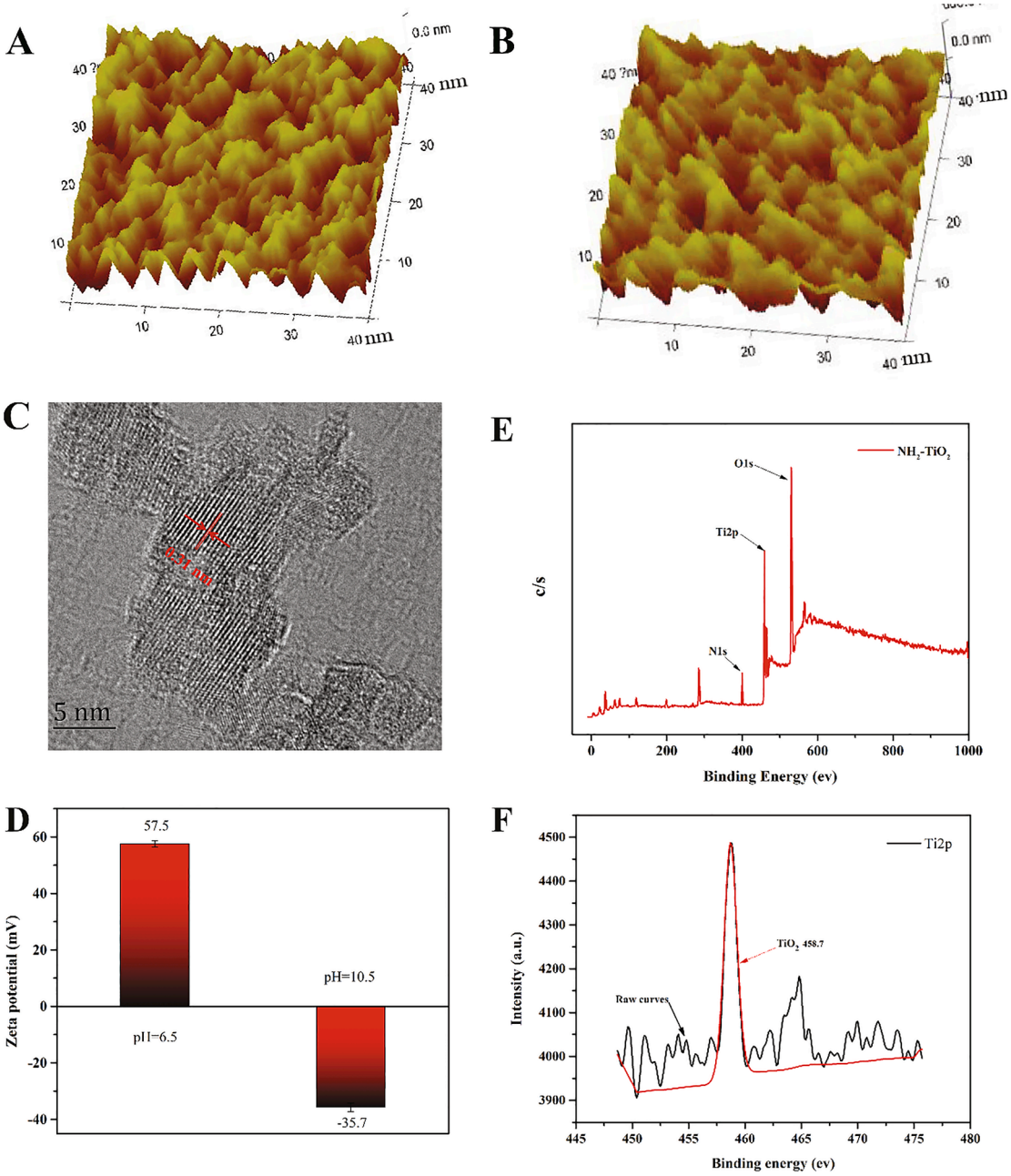

Fig. 1. The characterization of NH_2-TiO_2/MUA/AuE-QCM sensor. (A) bare electrode (AFM); (B) NH_2-TiO_2/MUA/AuE (AFM); (C) High resolution transmission electron microscopy (HR-TEM); (D) Zeta potential analysis; (E) and (F) X-ray photoelectron spectroscopy (XPS) spectra.

frequency of the NH_2-TiO_2/MUA/AuE electrode was stabilized. Then, 10 μL of the α-casein solution was carefully dropped onto the NH_2-TiO_2/MUA/AuE electrode surface and incubated for 20 min (equilibration time) at 4 °C. (The equilibration time of NH_2-TiO_2/MUA/AuE was shown in the supplementary material). The resulting frequency (Δfi, Hz) was recorded until the frequency change less than 1.0 Hz, regarding as the stable sensor response. The frequency shift Δf ($f_i - f_0$, Hz) was calculated, which was associated with mass change caused by the specific recognition of phosphoproteins. At least three parallel experiments were performed above. Average value of Δf was used to calculate the mass of phosphoproteins adsorbed onto the quartz crystal surface according to the Sauerbrey equation (Sauerbrey, 1959), (1):

$$\Delta f = -2.26 \times 10^{-6} \Delta m f_0^2 / A \quad (1)$$

where f_0 is the original frequency of the quartz crystal (Hz), Δm is the mass change (g), and A is the surface area of the electrode (cm^2).

The cyclic voltammetry measurement was performed to investigate the electron transmission procedure of the surface-modified electrodes in 1.0 mmol L^{-1} $K_3[Fe(CN)_6]$ aqueous solution containing 0.2 mol L^{-1} KNO_3 and with a scanned potential from −0.2 V to 0.6 V at the scan rate of 100 mV s^{-1}. NH_2-TiO_2/MUA/AuE electrodes modified with different layers step by step were detected in 5.0 mmol L^{-1} $K_3[Fe(CN)_6]$ solution containing 0.2 mol·L^{-1} KNO_3. All impedance data was acquired via electrochemical impedance spectroscopy (EIS). The detection conditions were that the frequency change range was 100 mHz ~ 100 kHz, the scanning point was 50, and the scan rate was 10 mV s^{-1}. All working electrodes (GCE, 4 mm diameter), reference electrode (saturated calomel electrode, SCE) and auxiliary electrode (platinum column electrode) were tested under the above conditions.

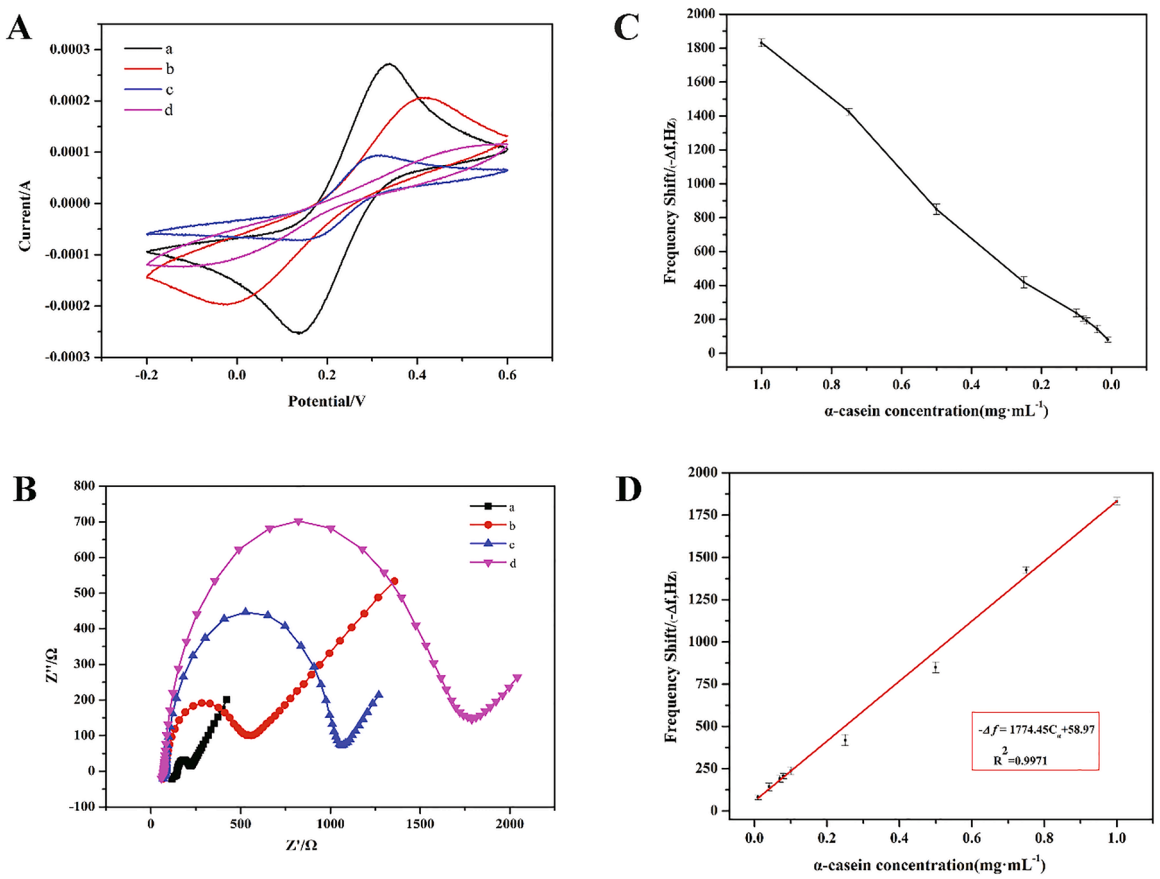

Fig. 2. (A) CV curves of different modified electrodes in $K_3[Fe(CN)_6]$ solution: (a) bare Au electrode, (b) 11-mercaptohexadecanoic acid, (c) NH_2-TiO_2/MUA/AuE (Blue), (d) phosphoproteins; (B) EIS of different modified electrodes in $K_3[Fe(CN)_6]/K_4[Fe(CN)_6]$ solution: (a) bare Au electrode, (b)11-mercaptohexadecanoic acid, (c) NH_2-TiO_2/MUA/AuE, (d) phosphoproteins; (C) The determination of α-casein concentration range; (D) Standard curve of the sensor. (For interpretation of the references to colour in this figure legend, the reader is referred to the web version of this article.)

2.5. Sample preparation

In this study, different sample matrixes (non-fat milk and the chicken egg white) were prepared.

(A) Pre-processing process of non-fat milk: 4 mL of the non-fat milk (protein content 3%) purchased from a local supermarket was centrifuged at 5,000 rpm for 30 min at 4 °C and then the fat layer was removed. The treated milk was diluted 5 times, 10 times, 15 times, and 20 times with NH_4HCO_3 solution (50 $mmoL^{-1}$, pH 6.5) and then kept in 4 °C refrigerator for use.

(B) The chicken egg white was obtained from fresh shell eggs bought from the TESCO supermarket (Tianjin). The egg whites were treated according to the reported method (Duan et al., 2019). Chicken egg white was diluted to 50% (v/v) with phosphate buffer (20 mM, pH 8.0). The diluted egg white solution was stirred in ice bath for 30 min, then centrifuged at 4 °C and 3000 $rpm{\cdot}min^{-1}$ for 10 min. The supernatant was used as the source of proteins.

3. Results and discussion

3.1. Characterization of NH_2-TiO_2/MUA/AuE

3.1.1. Morphological characterization of the AuE and NH_2-TiO_2/MUA/AuE

AFM was performed to visually show the morphological characteristics of AuE and NH_2-TiO_2/MUA/AuE. As shown in Fig. 1B, compared with AuE (Fig. 1A), the surface of NH_2-TiO_2/MUA/AuE showed a fibrous burr structure with a much rougher surface, which was possibly due to the good hydrophilicity and large specific surface area of aminated nano-titanium dioxide increasing the contact between 11-mercaptoundecanoic acid and NH_2-TiO_2. The morphological change of the electrode indicated that the aminated nano-titanium dioxide had been successfully modified on the electrode, which also largely explained the specific recognition sites existed on the electrode surface.

In addition, we characterized the nature of NH_2-TiO_2 nanoparticle by High resolution transmission electron microscopy (HR-TEM), X-ray photoelectron spectroscopy (XPS) and Zeta potential analysis. HR-TEM was used to demonstrated the detailed microstructures of the obtained nano NH_2-TiO_2. The HR-TEM image (Fig. 1C) showed a clear lattice fringes of 0.31 nm and could be assigned to the (011) plane of nano NH_2-TiO_2. The nano NH_2-TiO_2 as the substrate and specific recognition element can provide larger surface areas to load on AuE, which is beneficial for facilely capturing the α-casein.

Zeta potentials, electromotive potential, is used to directly measure the surface potential of nanoparticles and further evaluate the stability of the prepared particles (Crundwell, 2016; Lai, Deng, Wen, & Liu, 2019). Fig. 1D shows the zeta potential of nano NH_2-TiO_2 under acidic conditions (pH = 6.5) and alkaline conditions (pH = 10.5), respectively. Indeed, the zeta potential of NH_2-TiO_2 at pH 6.5 has a positive charge (ζ = +57.5 mV) (a), while that of the NH_2-TiO_2, as a Lewis base, were −35.7 mV (b). The zeta potential results shown above futher proved the separation and adsorption mechanism between the TiO_2 and the phosphoproteins.

XPS was employed to further investigate the elemental composition of NH_2-TiO_2 existing on the surface of the prepared NH_2-TiO_2/MUA/AuE-QCM and the results were shown in Fig. 1E and F. The results of

wide scan XPS show NH_2-TiO_2 that mainly consist of N, O and Ti, which means the N just only from -NH_2. The presence of N1s and Ti2p was further confirmed the successful decoration of NH_2-TiO_2 with good hydrophilia instead of TiO_2.

3.1.2. Electrochemical behavior of the sensor

Cyclic voltammetry (CV) is an effective and convenient method to investigate the electron transmission procedure of the surface-modified electrodes. In this work, various modified electrodes were monitored in 1.0 mmol·L^{-1} $K_3[Fe(CN)_6]$ solution containing 0.2 mol·L^{-1} KNO_3 by CV (Fang, Liu, Yang, & Wang, 2016). As shown in Fig. 2A, the cyclic voltammogram of bare AuE showed a couple of redox peaks (curve a). When the electrode surface was covered with the 11-mercaptohexadecanoic acid, the redox peak current in CV curve was significantly reduced (curve b). It decreased from 271.63 μA (bare electrode) to 206.05 μA. A lower peak current of electrode modified with aminated nano-titanium dioxide showed that the metal oxide hindered the electron transfer (curve c). In addition, it was seen the current response value (104.52 μA) of the electrode adsorbed with phosphoproteins was lower than the value (114.36 μA) of NH_2-TiO_2/MUA/AuE (curve d), it should be for the binding of the phosphoproteins to the aminated nano-titanium dioxide prevented the diffusion of the potassium ferricyanide probe on the electrode surface.

Electrochemical impedance spectroscopy (EIS) is an effective electrochemical technique for monitoring the interface properties of surface-modified electrodes (Liu, Fang, Deng, & Wang, 2015). In this work, various modified electrodes were monitored in 5.0 mmol·L^{-1} $K_3[Fe(CN)_6]$ solution containing 0.2 mol·L^{-1} KNO_3 by EIS. It was seen from Fig. 2B, the EIS of MUA/AuE (curve b) exhibited powerful electron transfer resistance (Ret) to the redox of the probe $K_3[Fe(CN)_6]$ (551 Ω) which was much larger than bare GCE (225 Ω curve a). The charge-transfer resistance for NH_2-TiO_2/MUA/AuE (curve c) showed an increase due to the weaked effect of non-conductive TiO_2 for conductivity of electrode. Ret of NH_2-TiO_2-MUA assembled electrode obviously increases to 1075 Ω (curve c), indicating that non-conducting metal oxide blocked the penetration of the redox probe. Ret of the modified electrode increased gradually after layer-by-layer assembly by coating NH_2-TiO_2, BSA as well as phosphoproteins specifically binded to the sites of titanium dioxide (curve d in Fig. 1D) on account of intrinsic non-conductivity of proteins. The characterizations shown above implied that each modification layer was validly immobilized on the electrode and the NH_2-TiO_2/MUA/AuE had been fabricated successfully.

3.2. Optimization of conditions for NH_2-TiO_2/MUA/AuE preparation

3.2.1. Selection of buffer NH_4HCO_3 solution pH

The pH of buffer NH_4HCO_3 solution is a critical factor that influences the activity of the phosphoproteins and further influences the adsorption performance of the aminated nano titanium dioxide film.

In general, the acidity coefficient (pKa) of 11-mercaptoundecanoic acid is 3.5 and the isoelectric points (pI) of α-casein and β-casein were 4.1 and 4.5 respectively (Huang, Wang, Wang, Liu, & Wang, 2015). The pH (4.1) of the solution is greater than the surface of the quartz crystal gold electrode pKa (3.5), so that the surface of the quartz crystal gold electrode will be negatively charged at this time. Since the phosphoprotein has a negative charge, it cannot be electrostatically adsorbed on the quartz crystal gold electrode surface. When the solution pH is greater than pI, the surface of quartz crystal gold electrode is still negatively charged, which can't adsorb phosphoproteins. Almost all proteins have isoelectric points below 6.5 (BSA: 4.9; γ-casein: 5.8–6.0; serum albumin: 4.7–4.9; β-lacto-globulin: 5.1–5.3, etc.) and casein will denature at pH less than 6.0 (Corredig, Nair, Li, Eshpari, & Zhao, 2019; Taterka & Castillo, 2015; Wang et al., 2017). Therefore, in this work, the pH of the selected buffer is in the range of 6.5 to 9.0 (pH > pI). Thus, the protein does not undergo static adsorption on the surface of the quartz crystal gold electrode but also ensures the activity of the protein. Fig. S1 shows the principle of electrode pre-binding experiment.

In this study, the pH of NH_4HCO_3 (50 mmoL·L^{-1}) buffer solution was 6.5, 7.0, 7.5, 8.0, 8.5, and 9.0 respectively. 10 μL of aminated nano titanium dioxide solution was added to the activated quartz crystal gold electrode and reacted for 20 min under nitrogen conditions. Then, the quartz crystal gold electrode was washed twice with ultrapure water and dried with nitrogen. Finally, the optimal pH for adsorption of phosphoproteins was determined based on the value of the frequency change (Δf, -Hz). The frequency shift showed a downward trend with the increment of pH from 6.5 to 9.0 and then reached a plateau after 8.0 (shown in Fig. S2). The reason was mainly attributed to that the repulsion between the negatively charged phosphoproteins and TiO_2, in which TiO_2 is negatively charged as a Lewis base under alkaline conditions. The corresponding variations of the frequency response were also recorded by QCM-sensor. Hence, 6.5 was considered as optimal adsorption pH.

3.2.2. Optimization of NH_2-TiO_2 addition

Moreover, the addition of NH_2-TiO_2 can influence the number of the phosphoprotein specific binding sites on sensor electrodes and further affect the sensitivity of the sensor. In the experiment, the optimal amount of NH_2-TiO_2/MUA/AuE-QCM sensor was determined by adding consecutive additions of NH_2-TiO_2 solution (0.25, 0.5, 0.75, 1, 1.25, 1.5, 1.75, 2.0 mg·mL^{-1}). It was found that the frequency shifts of the NH_2-TiO_2/MUA-Au electrode under the same conditions increased with the addition of NH_2-TiO_2 to a maximum at 10 μg. Excessive NH_2-TiO_2 resulted in a decrease of the frequency shift and then reached a plateau after 12.5 μg (Fig. S3). The reason may be that there were not enough effective adsorption sites on the electrode surface when the dropping amount was less than 10 μg. In contrast, superfluous NH_2-TiO_2 could induce the formation of thick rigid film layer, leading to the reduction of mass transfer rate and sensitivity of QCM sensor (Eriksson et al., 2013). The sensor prepared at the addition of 10 μg NH_2-TiO_2 exhibited the largest frequency shift during analysis. Thus, in the following experiments the addition of NH_2-TiO_2 was maintained at 10 μg.

3.3. Analytical performance of NH_2-TiO_2/MUA/AuE-QCM sensor

3.3.1. Piezoelectric frequency response at different α-casein concentrations

In order to investigate the adsorption capacity of NH_2-TiO_2/MUA/AuE-QCM sensor for the phosphoproteins, different concentrations of α-casein (4 °C, 0–1 mg·mL^{-1}) (Qi, Mao, Lu, Deng, & Zhang, 2010; Wei & Wang, 2017) was tested and the results were shown in Fig. 2C. The binding affinity of α-casein to the established sensor was evaluated by measuring the change in frequency response upon different concentration of α-casein solution. With the decrease of α-casein concentration, more specific recognition sites were empty, and the frequency response reduced accordingly. When the α-casein concentration was 1 mg mL^{-1}, the frequency shift reached 1831.87 Hz, which could be attributed to increased occupation of the specific sites by α-casein. Moreover, the frequency changes were slight for the NH_2-TiO_2/MUA/AuE electrode in the concentration range of 0.001 mg mL^{-1} to 0.03 mg mL^{-1}. All these results indicated that the frequency shifts were positively correlated with the concentration of α-casein.

3.3.2. Evaluation of binding performance

In this study, the binding affinity of phosphoproteins to the established sensor was evaluated by measuring the changes in frequency response upon consecutive additions of α-casein solution. With the increase of α-casein concentration, more specific sites were binded and the frequency response reduced accordingly. The results in Fig. 2D showed that the frequency shift was directly proportional to the concentration of α-casein ranging from 0.001 mg mL^{-1} to 1.0 mg mL^{-1} with a detection limit of 5.3×10^{-6} mg mL^{-1} (S/N = 3), the limit of quantitation was 0.001 mg mL^{-1}. The linear regression equation was expressed as $-\Delta f$ (Hz) = $1774.45C_\alpha + 58.97$($R^2 = 0.9971$). The frequency shift range and

Table 1
Comparison of different methods for the determination of phosphoproteins/phosphopeptides.

Methods	Characteristics	Sensitivity(μmol L^{-1})	Detection time (min)	Samples	Ref.
Ti^{4+}-IMAC	Large surface area, hydrophilicity, magneticseparation	–	60	β-casein/BSA(1:200),human serum	(Wang et al., 2014)
Fe^{3+}-IMAC	Nanomaterial: large surface area	0.5×10^{-7}	75	Nonfat milk; egg yolk; human serum	(Hussain et al., 2013)
TiO_2-MOAC	Mesomaterial: large surface area	0.3×10^{-9}	50	β-casein/BSA (1:100); nonfat milk; rat liver	(Zhang et al., 2012)
ZrO_2.GCE	large surface area	0.0934	–	–	(Gao et al., 2016)
NH_2-TiO_2/MUA/ AuE-QCM	Nanomaterial Large surface area, hydrophilicity	0.0002	5	nonfat milk; chicken egg white;α-casein/ BSA (1:1000)	This work

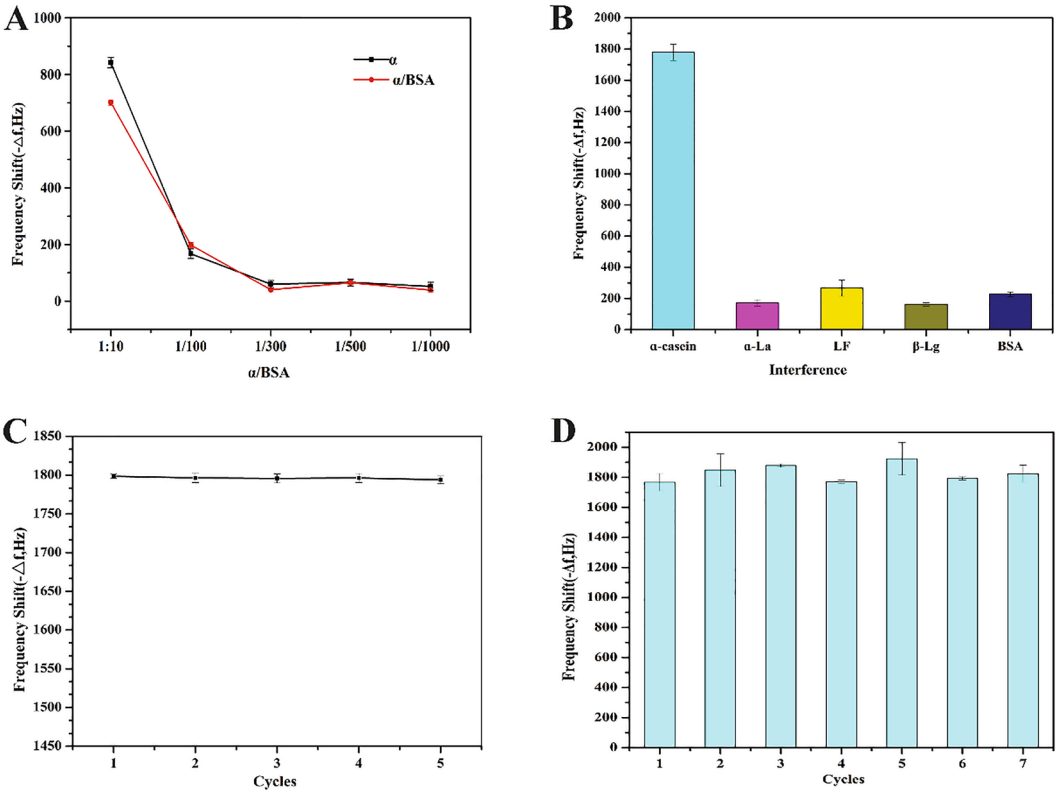

Fig. 3. (A) The frequency shift corresponding to the NH_2-TiO_2/MUA/AuE for only α-casein and α/BSA analytes at different ratios; (B) Selectivity of the NH_2-TiO_2/MUA/AuE to α-casein and some non-phosphoproteins with the same concentration; (C) Influence of the repeatability cycles on α-casein adsorption using NH_2-TiO_2/MUA/AuE; (D) The stability of the NH_2-TiO_2/MUA/AuE to α-casein.

linear range obtained from NH_2-TiO_2/MUA/AuE were broad.

3.4. Analysis time and selectivity capability experiment

The adsorption static of developed QCM sensor towards phosphoproteins (α-casein) at a concentration of 1 mg mL^{-1} was studied and shown in Fig. S4. Because of the large specific surface area, high specificity and good hydrophilic of NH_2-TiO_2, NH_2-TiO_2/MUA- QCM sensor exhibited a steady frequency shift within 5 min. Compared with other reported measures (listed in Table 1), the fabricated NH_2-TiO_2/MUA/AuE-QCM sensor in this study was quick and had a good sensitivity. The short analysis time was helpful for the rapid detection.

The selectivity of the NH_2-TiO_2/MUA/AuE electrode was also evaluated in this study. A selective experiment was carried out to evaluate the recognition capability of proposed sensor. α-Casein and a series of α-casein/BSA (concentration ratio of α-casein/BSA: 1:10, 1:100, 1:300, 1:500, 1:1000) were tested, respectively. The results in Fig. 3A showed that the frequency shifts were almost consistent by comparing the frequency shift of α-casein at the same concentration (Fig. 3A black curve). This result validated that the NH_2-TiO_2/MUA/AuE sensor was significantly better than BSA in its ability to select and recognize phosphoproteins. In addition, α-casein and some non-phosphoproteins at the same concentration of 1 mg·mL^{-1} were tested, including lactoferrin (LF), lacto-globulin (β-Lg), whey protein (α-La), bovine serum albumin (BSA) respectively, and the results were shown in Fig. 3B. The frequency shifts for the non-phosphoproteins LF, β-Lg, α-La and BSA were much less significant than for the α-casein, indicating the good selectivity of the NH_2-TiO_2/MUA/AuE to α-casein. Therefore, the constructed NH_2-TiO_2/MUA/AuE had a good selectivity for phosphoproteins.

3.5. Reproducibility and stability of NH_2-TiO_2/MUA/AuE

Stability and reproducibility of the developed QCM sensor were evaluated. Fig. 3C showed the relative standard deviation (RSD) of the frequency shifts signal for 1 mg mL^{-1} α-casein was 4.2% under

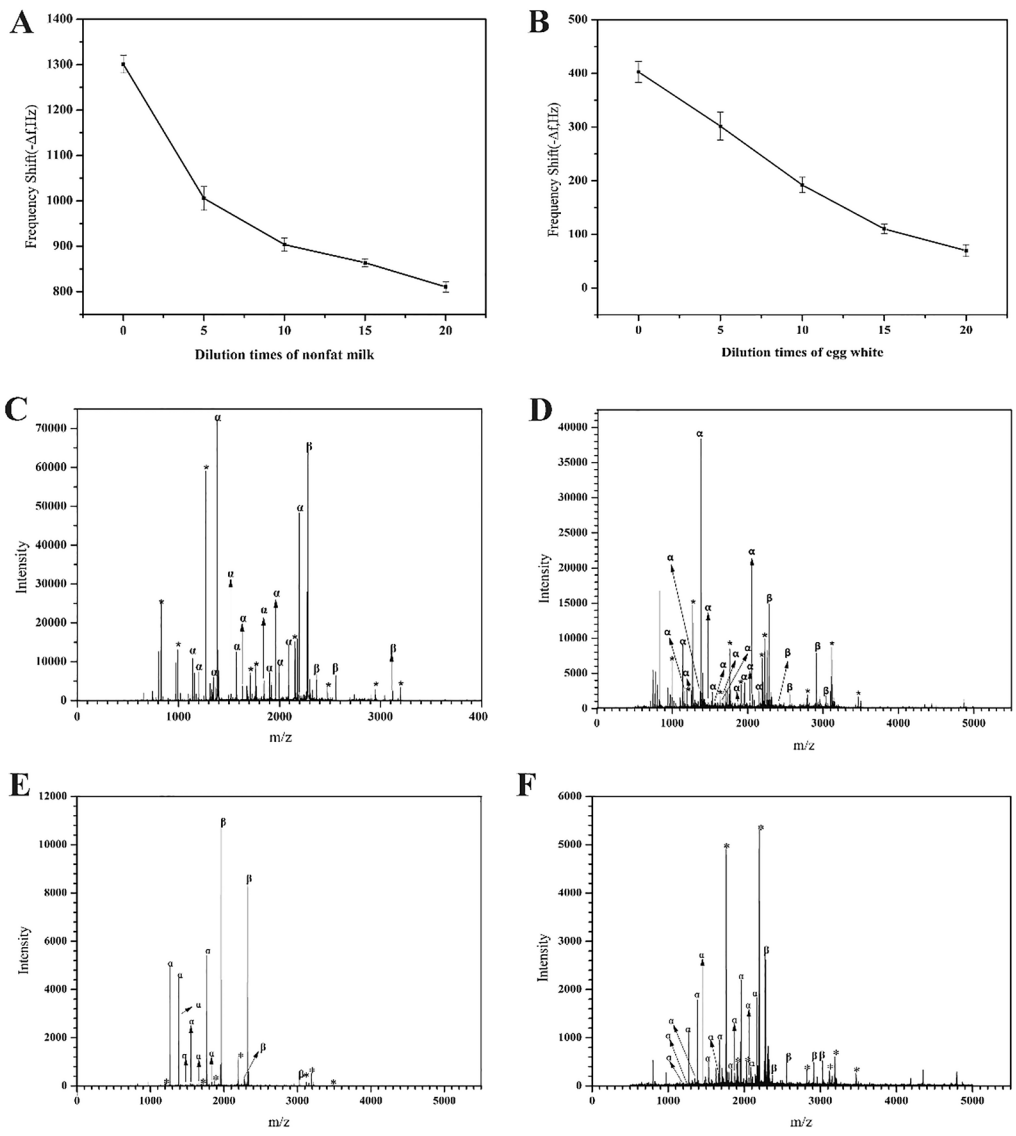

Fig. 4. (A) Frequency shift of the actual sample nonfat milk; (B) Frequency shift of the actual sample egg white; (C) MALDI-TOF MS spectra of phosphopeptides from the trypsin hydrolysate of α-casein eluted from the electrode; (D) MALDI-TOF MS spectra of phosphopeptides from the trypsin hydrolysate of β-casein eluted from the electrode; (E) MALDI-TOF MS spectra of phosphopeptides from the trypsin hydrolysate of nonfat milk eluted from the electrode; (F) MALDI-TOF MS spectra of phosphopeptides from the trypsin hydrolysate of mixture (casein) eluted from the electrode. (*dephosphorylated fragment).

continuous five parallel experiments, indicating the QCM sensor having outstanding stability and reliability. In order to evaluate the reproducibility of QCM sensor, five pretreated NH_2-TiO_2/MUA/AuE were measured after incubating at 1 mg mL^{-1} α-casein solution, the RSD of the frequency shifts was 6.8%. The above results revealed that the proposed sensor had favorable reproducibility during preparation and measurement.

To evaluate the long-term preservation stability of the proposed sensor, the frequency shifts of NH_2-TiO_2/MUA/AuE toward 1.0 mg mL^{-1} α-casein solution was measured and recorded weekly. The results in Fig. 3D revealed that the frequency shifts presented a slight change and the sensor maintained more than 90% response efficiency after being stored at room temperature for a month. The good reproducibility and stability of the developed QCM sensor were attributed to the good stability of NH_2-TiO_2 metal oxide and rigid structure of the NH_2-TiO_2/MUA film.

3.6. Application of the QCM sensor in practical samples

In order to demonstrate the applicability and feasibility of the NH_2-TiO_2/MUA/AuE-QCM sensor, phosphoproteins in non-fat milk, egg white were tested by adsorption experiments. The statistical results were shown in Fig. 4A, the frequency shifts of NH_2-TiO_2/MUA/AuE-QCM sensor were different for the adsorption of phosphoproteins in different dilutions of non-fat milk. The frequency shifts (-Δ*f*, Hz) decreased with the increase of the dilution of non-fat milk. The frequency shifts (-Δ*f*, Hz) reached the maximum value of 1301.2 Hz without dilution of centrifuged nonfat milk and the quality of phosphoproteins were 8.932×10^{-1} μg. The adsorption of phosphoproteins in different dilutions of egg white by NH_2-TiO_2/MUA/AuE-QCM sensor was shown in Fig. 4B. The smaller the frequency change value (−Δ*f*), the greater the egg white dilution. When the egg white was not diluted by NH_4HCO_3 buffer, the frequency change value (-Δ*f*) of the sensor reached a maximum of 402.7 Hz, and the mass of the phosphoproteins were 2.764×10^{-1} μg. These results proved that the NH_2-TiO_2/MUA/AuE-QCM sensor can be applied to the accurate detection and effective analysis of trace the phosphoproteins in actual samples.

3.7. MALDI-TOF MS qualitative validation

In order to further verify the detection accuracy of the constructed sensor, the trypsin hydrolysate of phosphoproteins eluted from the electrode were detected by the MALDI-TOF mass spectrum. The mass spectrum analysis was performed for trypsin hydrolysate of α-casein (Fig. 4C) and β-casein (Fig. 4D) in which the α-casein and β-casein were collected from the chips of the prepared sensor after being eluted with

15% aqueous ammonia (10 μL). The mass spectrum analysis based on MALDI-TOF revealed that the peaks were dominated by strong signals from the phosphopeptides. This result further demonstrated that the NH_2-TiO_2/MUA/AuE piezoelectric sensor had a high specific selectivity for phosphoproteins.

To demonstrate that the NH_2-TiO_2/MUA/AuE-QCM sensor has good adsorption capacity for phosphorylated proteins in the actural sample, we further carried out the same verificatory experiments on complex samples (e.g. casein and non-fat milk). The mass spectrograms (Fig. 4E and F) were the trypsin hydrolysate of phosphoproteins eluted with 15% aqueous ammonia from sensor. The analysis results of the trypsin hydrolysate of non-fat milk and mixture (casein) were displayed in Fig. 4E and F, respectively. It was reported (Baker et al., 2011) that only 3 phosphopeptides can be detected by mass spectrometry when the phosphopeptides was not enriched. In contrast, the proposed sensor can detect more phosphopeptides and the detection method was more sensitive. These results proved the NH_2-TiO_2/MUA/AuE-QCM sensor has practical significance for the selective adsorption and rapid detection of trace phosphoproteins from real samples.

4. Conclusion

In summary, a novel based NH_2-TiO_2/MUA/AuE-QCM sensor for rapid determination of trace phosphoproteins had been successfully constructed by self-assembly onto 11-mercaptoundecanoic acid decorated AuE surface for the first time. The QCM sensor had advantages of large specific surface area, high specificity and good hydrophilic of NH_2-TiO_2, higher sensitivity and shorter analysis time. Under optimal conditions, the proposed QCM sensor using NH_2-TiO_2/MUA/AuE as working electrode rapidly selectively recognized trace phosphoproteins under a complex system. The QCM sensor had ability to achieve linear detection of α-casein from 1.0×10^{-3} to 1.0 mg mL^{-1} with a LOD of 5.3×10^{-6} mg mL^{-1} and LOQ of 1.0×10^{-3} mg mL^{-1}. Moreover, repeated measurements and long-term storage hardly affected the stability of the proposed sensor. More importantly, the proposed sensor was successfully applied for detecting trace phosphoproteins in non-fat milk and egg white, making it possible to detect trace phosphoproteins in actual samples. The experimental results had good correlation with the MALDI-TOF MS detection results, which showed that the QCM sensor had a good application prospect for rapid detection of phosphoproteins.

CRediT authorship contribution statement

Jianping Guo: Methodology, Investigation, Writing - original draft. **Guozhen Fang:** Conceptualization. **Shuo Wang:** Conceptualization. **Junping Wang:** Supervision, Conceptualization, Writing - review & editing.

Declaration of Competing Interest

The authors declare that they have no known competing financial interests or personal relationships that could have appeared to influence the work reported in this paper.

Acknowledgements

This work was supported by "The National Key R&D Program of China" (No. 2016YFD0401202); The Open Project of the State Key Laboratory of Food Nutrition and Safety in 2020-2021 (SKLFNS-KF-202010) and the Special Project of Tianjin Innovation Platform (No.17PTGCCX00230).

Appendix A. Supplementary data

Supplementary data to this article can be found online at https://doi.org/10.1016/j.foodchem.2020.128656.

References

Altintas, Z., Uludag, Y., Gurbuz, Y., & Tothill, I. (2012). Development of surface chemistry for surface plasmon resonance based sensors for the detection of proteins and DNA molecules. *Analytica Chimica Acta, 712*, 138–144.

Avila, M., Zougagh, M., Escarpa, A., & Rios, A. (2007). Supported liquid membrane-modified piezoelectric flow sensor with molecularly imprinted polymer for the determination of vanillin in food samples. *Talanta, 72*(4), 1362–1369.

Baker, M. A., Smith, N. D., Hetherington, L., Pelzing, M., Condina, M. R., & Aitken, R. J. (2011). Use of titanium dioxide to find phosphopeptide and total protein changes during epididymal sperm maturation. *Journal of Proteome Research, 10*(3), 1004–1017.

Chen, M., Wang, L., Qian, H., Zhang, H., Li, Y., Wu, G., et al. (2019). The effects of phosphate salts on the pasting, mixing and noodle-making performance of wheat flour. *Food Chemistry, 283*, 353–358.

Chen, I. H., Xue, L., Hsu, C. C., Paez, J. S., Pan, L., Andaluz, H., et al. (2017). Phosphoproteins in extracellular vesicles as candidate markers for breast cancer. *Proceedings of the National Academy of Sciences of the United States of America, 114*(12), 3175–3180.

Corredig, M., Nair, P. K., Li, Y., Eshpari, H., & Zhao, Z. (2019). Invited review: Understanding the behavior of caseins in milk concentrates. *Journal of Dairy Science, 102*(6), 4772–4782.

Dai, J., Wang, M., & Liu, H. (2017). Highly selective enrichment of phosphopeptides using Zr(4+)-immobilized Titania nanoparticles. *Talanta, 164*, 222–227.

Ding, P., Liu, R., Liu, S., Mao, X., Hu, R., & Li, G. (2013). Reusable gold nanoparticle enhanced QCM immunosensor for detecting C-reactive protein. *Sensors and Actuators B: Chemical, 188*, 1277–1283.

Duan, H. L., Niu, Q. L., Wang, J., Ma, S. Y., Zhang, J., & Zhang, Z. Q. (2019). High uptake carboxyl-functionalized porous beta-cyclodextrin polymer for selective extraction of lysozyme from egg white. *Journal of Chromatography A, 1600*, 80–86.

Enomoto, H., Li, C. P., Morizane, K., Ibrahim, H. R., Sugimoto, Y., Ohki, S., et al. (2007). Glycation and phosphorylation of beta-lactoglobulin by dry-heating: Effect on protein structure and some properties. *Journal of Agriculture and Food Chemistry, 55*(6), 2392–2398.

Eriksson, A. I., Bartsch, M., Bergquist, J., Edwards, K., Lind, S. B., & Agmo Hernandez, V. (2013). On-target titanium dioxide-based enrichment for characterization of phosphorylations in the Adenovirus pIIIa protein. *Journal of Chromatography A, 1317*, 105–109.

Fang, G., Liu, G., Yang, Y., & Wang, S. (2016). Quartz crystal microbalance sensor based on molecularly imprinted polymer membrane and three-dimensional Au nanoparticles@mesoporous carbon CMK-3 functional composite for ultrasensitive and specific determination of citrinin. *Sensors and Actuators B: Chemical, 230*, 272–280.

Gao, F.-F., Wang, Y.-B., Wang, K., & Xia, X.-H. (2016). Competitive approach to the electrochemical detection of phosphopeptides on a porous ZrO_2 thin film electrode. *Journal of Electroanalytical Chemistry, 781*, 97–102.

Gruhler, A., Olsen, J. V., Mohammed, S., Mortensen, P., Faergeman, N. J., Mann, M., et al. (2005). Quantitative phosphoproteomics applied to the yeast pheromone signaling pathway. *Molecular and Cellular Proteomics, 4*(3), 310–327.

Haupt, K., Medina Rangel, P. X., & Bui, B. T. S. (2020). Molecularly imprinted polymers: antibody mimics for bioimaging and therapy. *Chemical Reviews, 120*(17), 9554–9582.

Hong, Y., Zhan, Q., Pu, C., Sheng, Q., Zhao, H., & Lan, M. (2018). Highly efficient enrichment of phosphopeptides from HeLa cells using hollow magnetic macro/mesoporous TiO_2 nanoparticles. *Talanta, 187*, 223–230.

Huang, X., Wang, J., Wang, J., Liu, C., & Wang, S. (2015). Preparation of graphene–hafnium oxide composite for selective enrichment and analysis of phosphopeptides. *RSC Advances, 5*(109), 89644–89651.

Hunter, T. (1995). Protein kinases and phosphatases: The Yin and Yang of protein phosphorylation and signaling. *Cell, 80*(2), 225–236.

Hussain, D., Najam-ul-Haq, M., Jabeen, F., Ashiq, M. N., Athar, M., Rainer, M., et al. (2013). Functionalized diamond nanopowder for phosphopeptides enrichment from complex biological fluids. *Analytica Chimica Acta, 775*, 75–84.

Kong, L. J., Pan, M. F., Fang, G. Z., He, X. L., Yang, Y. K., Dai, J., et al. (2014). Molecularly imprinted quartz crystal microbalance sensor based on poly(o-aminothiophenol) membrane and Au nanoparticles for ractopamine determination. *Biosensors & Bioelectronics, 51*, 286–292.

Lebetwa, N., Suzuki, Y., Tanaka, S., Nakamura, S., & Katayama, S. (2019). Enhanced anti-allergic activity of milk casein phosphopeptide by additional phosphorylation in ovalbumin-sensitized mice. *Molecules, 24*(4).

Li, C.-P., Chen, D., Peng, J., Enomoto, H., Hayashi, Y., Li, C., et al. (2010). Improvement of functional properties of whey soy protein phosphorylated by dry-heating in the presence of pyrophosphate. *LWT – Food Science and Technology, 43*(6), 919–925.

Li, C.-P., Enomoto, H., Hayashi, Y., Zhao, H., & Aoki, T. (2010). Recent advances in phosphorylation of food proteins: A review. *LWT – Food Science and Technology, 43*(9), 1295–1300.

Liu, H., Fang, G., Deng, Q., & Wang, S. (2015). A triple-dimensional sensing chip for discrimination of eight antioxidants based on quantum dots and graphene. *Biosensors & Bioelectronics, 74*, 313–317.

Lu, Z., Duan, J., He, L., Hu, Y., & Yin, Y. (2010). Mesoporous $TiO_{(2)}$ nanocrystal clusters for selective enrichment of phosphopeptides. *Analytical Chemistry, 82*(17), 7249–7258.

Ma, W. F., Zhang, Y., Li, L. L., You, L. J., Zhang, P., Zhang, Y. T., et al. (2012). Tailor-made magnetic Fe_3O_4@mTiO_2 microspheres with a tunable mesoporous anatase shell for highly selective and effective enrichment of phosphopeptides. *ACS Nano, 6*(4), 3179–3188.

Manning, G., Whyte, D. B., Martinez, R., Hunter, T., & Sudarsanam, S. (2002). The protein kinase complement of the human genome. *Science, 298*(5600), 1912–1934.

Pan, M., Kong, L., Liu, B., Qian, K., Fang, G., & Wang, S. (2013). Production of multi-walled carbon nanotube/poly(aminoamide) dendrimer hybrid and its application to piezoelectric immunosensing for metolcarb. *Sensors and Actuators B: Chemical, 188*, 949–956.

Qi, D., Mao, Y., Lu, J., Deng, C., & Zhang, X. (2010). Phosphate-functionalized magnetic microspheres for immobilization of $Zr^{(4+)}$ ions for selective enrichment of the phosphopeptides. *Journal of Chromatography A, 1217*(16), 2606–2617.

Sauerbrey, G. (1959). Verwendung von Schwingquarzen zur Wägung dünner Schichten und zur Mikrowägung. *Zeitschrift fur Physik, 155*(2), 206–222.

Say, R., Gultekin, A., Ozcan, A. A., Denizli, A., & Ersoz, A. (2009). Preparation of new molecularly imprinted quartz crystal microbalance hybride sensor system for 8-hydroxy-2'-deoxyguanosine determination. *Analytica Chimica Acta, 640*(1–2), 82–86.

Taterka, H., & Castillo, M. (2015). The effect of whey protein denaturation on light backscatter and particle size of the casein micelle as a function of pH and heat-treatment temperature. *International Dairy Journal, 48*, 53–59.

Tramutola, A., Lanzillotta, C., Perluigi, M., & Butterfield, D. A. (2017). Oxidative stress, protein modification and Alzheimer disease. *Brain Research Bulletin, 133*, 88–96.

Twisk, F. (2013). Rebuttal to Ickmans et al. association between cognitive performance, physical fitness, and physical activity level in women with chronic fatigue syndrome. J Rehabil Res Dev. 2013;50(6):795-810. www.rehab.research.va.gov/jour/ 2013/506/pdf/ickmans506.pdf. J Rehabil Res Dev, 50(9), vii-viii.

Wang, L., Ma, Y., Cui, J., Oyeyinka, S. A., Cheng, J., & He, S. (2017). Yak milk whey protein denaturation and casein micelle disaggregation/aggregation at different pH and temperature. *International Dairy Journal, 71*, 131–135.

Wang, Z.-G., Zhang, J.-L., Sun, D.-H., & Ni, J.-Z. (2014). Novel Ti^{4+}-chelated magnetic nanostructured affinity microspheres containing N-methylene phosphonic chitosan for highly selective enrichment and rapid separation of phosphopeptides. *Journal of Materials Chemistry B, 2*(39), 6886–6892.

Wei, X. N., & Wang, H. L. (2017). Facile fabrication of hydrophilic PAA-Ti/TiO_2 nanocomposite for selective enrichment and detection of phosphopeptides from complex biological samples. *Analytica Chimica Acta, 949*, 67–75.

Yu, L., Yang, W., Sun, J., Zhang, C., Bi, J., & Yang, Q. (2015). Preparation, characterisation and physicochemical properties of the phosphate modified peanut protein obtained from Arachin Conarachin L. *Food Chemistry, 170*, 169–179.

Zanivan, S., Gnad, F., Wickström, S. A., Geiger, T., Macek, B., Cox, J., et al. (2008). Solid tumor proteome and phosphoproteome analysis by high resolution mass spectrometry. *Journal of Proteome Research, 7*(12), 5314–5326.

Zhang, H., Hou, J., Cui, R., Guo, X., Shi, Z., Yang, F., et al. (2013). Phosphoproteome analysis reveals an important role for glycogen synthase kinase-3 in perfluorododecanoic acid-induced rat liver toxicity. *Toxicology Letters, 218*(1), 61–69.

Zhang, L., Liang, Z., Yang, K., Xia, S., Wu, Q., Zhang, L., et al. (2012). Mesoporous TiO_2 aerogel for selective enrichment of phosphopeptides in rat liver mitochondria. *Analytica Chimica Acta, 729*, 26–35.

Zhao, X., He, Y., Wang, Y., Wang, S., & Wang, J. (2020). Hollow molecularly imprinted polymer based quartz crystal microbalance sensor for rapid detection of methimazole in food samples. *Food Chemistry, 309*, Article 125787.

Zhu, B., Zhou, Q., Zhen, D., Wang, Y., Cai, Q., & Chen, P. (2019). Preparation of TiO_2/Bi/Fe/Zr nanocomposite for the highly selective enrichment of phosphopeptides. *Talanta, 194*, 870–875.